Available online at www.sciencedirect.com
ScienceDirect
Applied Catalysis B: Environmental 81 (2008) 56–63
APPLIED CATALYSIS B: ENVIRONMENTAL
www.elsevier.com/locate/apcatb

Support effect on complete oxidation of volatile organic compounds over Ru catalysts

Tomohiro Mitsui, Kazuki Tsutsui, Toshiaki Matsui, Ryuji Kikuchi, Koichi Eguchi *

Department of Energy and Hydrocarbon Chemistry, Graduate School of Engineering, Kyoto University, Nishikyo-ku, Kyoto 615-8510, Japan

Received 5 October 2007; received in revised form 26 November 2007; accepted 11 December 2007
Available online 23 December 2007

Abstract

Catalytic combustion of ethyl acetate, acetaldehyde, and toluene was investigated on various supported Ru catalysts prepared by the impregnation method, and the effect of reduction treatment on the activity was examined. Among the as-calcined catalysts tested, Ru/CeO_2 showed the highest activity for all tests regardless of the pre-treatment in hydrogen atmosphere. The catalytic activity of Ru/SnO_2 was significantly degraded by the reduction treatment, whereas the activity of Ru/ZrO_2 and $Ru/\gamma\text{-}Al_2O_3$ was enhanced. To reveal these phenomena, the as-calcined and reduced catalysts were characterized by X-ray diffraction (XRD), X-ray photoelectron spectroscopy (XPS), temperature-programmed reduction (TPR), transmission electron microscopy (TEM), and BET surface area. The dispersion of ruthenium on the supports was evaluated by chemisorption methods of carbon monoxide. The catalytic activity was strongly related to ruthenium species easily oxidizable and reducible at low temperatures. Such ruthenium species were loaded on CeO_2 in a highly dispersed state, resulting in the highest activity.

Keywords: Volatile organic compounds; Catalytic combustion; Supported Ru catalysts; Reduction treatment

1. Introduction

Volatile organic compounds (VOCs) have relatively high-vapor pressure and thus easily vaporize under ambient conditions. VOCs are known to cause air pollution such as photochemical smog, ground-level ozone, sick house syndrome, and chemical sensitivity [1–3]. Various methods such as catalytic combustion, flame combustion, catalytic decomposition using ozone and plasma, photocatalytic decomposition, adsorbent-based methods, and so on, have been intensively investigated for effective abatement of VOCs [4–10]. Among these methods, catalytic combustion has advantageous features for VOCs removal: (i) complete combustion of dilute fuel proceeds stably at low temperatures; (ii) extremely low emission of NO_x and unburned fuels can be achieved [11].

In general, supported precious metal catalysts exhibit high activity for low-temperature oxidation of VOCs [12–17]. Among supported precious metal catalysts, Ru catalysts are known to be active for various catalytic reactions such as, e.g., water–gas shift reaction, ammonia synthesis, and reduction of NO by hydrocarbon [18–22]. A few studies have been conducted so far on VOC combustion over supported Ru catalysts, despite the various applications in the wide areas as mentioned above. Only wet air oxidation of VOCs has been conventionally carried out over supported Ru catalysts [23–25]. This method, however, needs highly pressurized conditions in order to oxidize VOCs at low temperatures, and is inappropriate for practical use. As an alternative, VOC oxidation in gas phase should be investigated under atmospheric pressure.

The aim of this work is to develop catalysts with high-combustion efficiency for VOCs at low temperatures. Several oxides supported ruthenium catalysts (Ru/oxide) were prepared, and catalytic oxidation of VOCs such as ethyl acetate, acetaldehyde, and toluene was examined. In addition, the influence of preparation conditions including reduction treatment on the catalytic activity was investigated.

2. Experimental

2.1. Catalyst preparation

Supported Ru catalysts were prepared by the impregnation method. The following oxides were selected as support

* Corresponding author. Tel.: +81 75 383 2519; fax: +81 75 383 2520.
E-mail address: eguchi@scl.kyoto-u.ac.jp (K. Eguchi).

0926-3373/$ – see front matter © 2008 Elsevier B.V. All rights reserved.
doi:10.1016/j.apcatb.2007.12.006

materials: SnO_2 (Wako Pure Chemical), CeO_2 (Aldrich), ZrO_2 (RC-100, Daiichi Kigenso Kagakukogyo), and γ-Al_2O_3 (JRC-ALO-8, The Catalysis Society of Japan). Tin oxide powder was calcined at 800 °C for 5 h prior to soaking, whereas others were used without any pre-treatments. Solution of $Ru(NO_3)_3$ (Tanaka Kikinzoku Kogyo) was used as a Ru source. Support materials were impregnated with the solution. The mixture was kept on a steam bath at 80 °C until the solvent was evaporated. Subsequently, the resulting powder was calcined at 400 °C for 30 min in air. Metal loading in the samples was 1.0 or 10 wt.% as in the metallic form. The catalysts with heavy loading were prepared to clarify the changes in crystalline phase and electronic state of precious metals. A part of as-calcined catalysts was heat-treated at 400 °C for 15 min in 50% H_2/N_2 prior to characterization and catalytic reactions.

2.2. Catalytic combustion of VOCs

A fixed-bed flow reactor made of quartz tubing of 8 mm inner diameter was used, and the prepared catalyst (600 mg) was set in the reactor. Each catalyst was tabletted and pulverized into 10–26 mesh before catalytic reaction tests. A gaseous mixture of VOCs and air was fed at a flow rate of 100 ml min^{-1} (space velocity: 10,000 l kg^{-1} h^{-1}). The outlet gas compositions were analyzed by an on-line micro-gas chromatograph with a thermal conductivity detector (TCD) (VARIAN, CP-4900) and a flame ionization detector (FID) (Shimadzu, GC-8A). For acetaldehyde and toluene combustion, the measurements were conducted during a heating process at 100 °C h^{-1}. In the case of ethyl acetate combustion, catalyst bed temperature was kept constant until the concentration of ethyl acetate and CO_2 at the outlet became stable.

2.3. Catalyst characterization

The samples were characterized by using the following equipments. X-ray diffraction (XRD) patterns were recorded by Cu Kα radiation on a RIGAKU Rint 2500 diffractometer for phase identification in the samples. X-ray photoelectron spectroscopy (XPS) measurements were conducted on Shimadzu ESCA-850 using a Mg Kα source. In the case of reduced catalysts, the samples were transferred directly into the XPS chamber without exposure to air after reduction treatment. Temperature-programmed reduction (TPR) measurements were performed in a quartz tube reactor, and the amount of consumed hydrogen was measured by a thermal conductivity detector (TCD). A weighed amount (25 mg) of the as-calcined catalyst was placed in the reactor, and then a gaseous mixture of 5% H_2–95% Ar was fed to the reactor at 30 ml min^{-1}. The temperature was raised to 800 °C at a heating rate of 10 °C min^{-1}. The dispersion of ruthenium on supports was determined by CO pulse method (Quantachrom CHEMBET 3000 system). Transmission electron microscopy (TEM) observation was carried out using a Hitachi H-9000 electron microscopy at an applied voltage of 300 kV. BET surface area was measured by N_2 adsorption at the liquid nitrogen temperature using a Shimadzu Gemini 2375 analyzer.

3. Results and discussion

3.1. Catalytic activity of VOC combustion

The catalytic activity of supported Ru catalysts for VOC combustion was significantly dependent on the support materials. The results of the combustion tests over as-calcined 1.0 wt.% Ru/SnO_2, Ru/ZrO_2, Ru/CeO_2, and Ru/γ-Al_2O_3 are shown in Fig. 1. The VOC conversion was calculated based

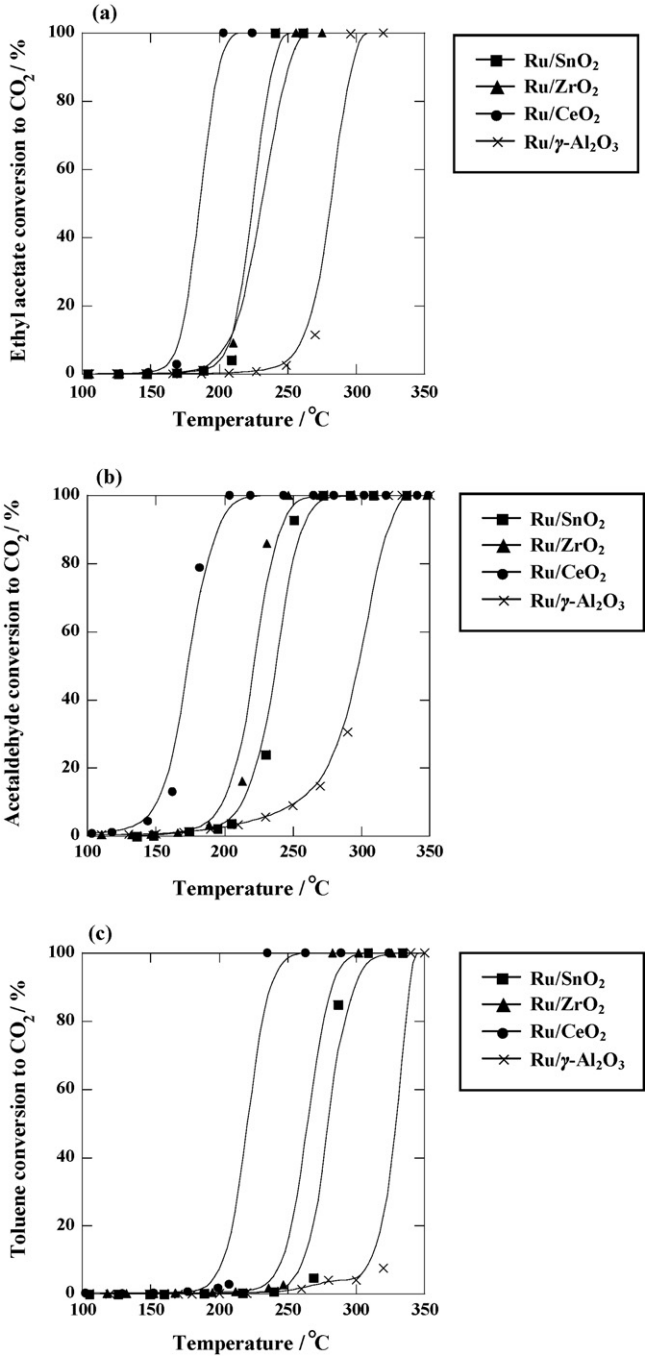

Fig. 1. VOC conversion as a function of temperature over supported 1.0 wt.% Ru catalysts: (a) ethyl acetate, (b) acetaldehyde, and (c) toluene. Reaction conditions: VOCs, 1.0%; air, 99.0%; S.V. = 10,000 l kg^{-1} h^{-1}.

Table 1
Physical properties of the as-calcined supported 1.0 wt.% Ru catalysts

Catalyst	BET surface area ($m^2\ g^{-1}$)	The amount of CO adsorbed (mmol g^{-1})	Particle size of Ru (nm)	Ru dispersion (%)
Ru/SnO_2	4.9	n.a.	–	–
Ru/ZrO_2	95	0.031	4.2	31.6
Ru/CeO_2	65	0.029	4.5	29.6
$Ru/\gamma\text{-}Al_2O_3$	141	0.020	6.5	20.7

n.a.: no adsorption.

on CO_2 concentration at reactor outlet. Among the catalysts, Ru/CeO_2 exhibited the highest activity for oxidation of various VOCs, and is more active for acetaldehyde combustion than Pd catalysts such as Pd/SnO_2 that we have previously reported [17]. The ignition temperature of toluene was higher than that of acetaldehyde and ethyl acetate, irrespective of the catalysts, indicating volatile aromatic compounds are less combustible. There was no clear correlation between the VOC conversion and the BET surface area (Table 1). It is noted that the activity of Ru/SnO_2 with the lowest surface area is comparable to that of Ru/ZrO_2, whereas $Ru/\gamma\text{-}Al_2O_3$ with high-surface area exhibited the lowest activity for all tests. This should be caused by the metal–support interaction. It should also be added that complete combustion of the VOCs was impossible over the supports alone. For ethyl acetate combustion, for example, many by-products such as acetaldehyde, ethanol, methane, hydrogen, and so on, were observed. On the other hand, the reduction treatment in a hydrogen atmosphere led to a significant change in the catalytic activity as shown in Fig. 2. The catalytic activity of Ru/ZrO_2 and $Ru/\gamma\text{-}Al_2O_3$ was enhanced, whereas that of Ru/SnO_2 was drastically degraded. As in the case of the as-calcined catalysts, Ru/CeO_2 exhibited the highest activity, which was almost unchanged before and after the reduction treatment. In these experiments, no correlation was also observed between the activity and the surface area. Thus, the effect of reduction treatment differs depending on supports, and details will be discussed in the following section.

3.2. Characterization of the supported Ru catalysts

3.2.1. Surface characterization

Surface characteristics of as-calcined catalysts are summarized in Table 1. The amount of CO adsorbed on Ru/SnO_2 and $Ru/\gamma\text{-}Al_2O_3$ was measured using the conventional CO pulse method after pre-treatment at 400 °C for 15 min in hydrogen atmosphere. For ruthenium dispersion on ZrO_2 and CeO_2 supports, O_2–CO_2–H_2–CO pulse method was adopted since the conventional method is ineffective for the supports with large oxygen storage capacity due to overestimation of CO adsorbed [26]. In the case of Ru/ZrO_2 and Ru/CeO_2, it was revealed that ruthenium particles were loaded on the supports in a highly dispersed state as compared with $Ru/\gamma\text{-}Al_2O_3$. This should result in the high-catalytic activity of Ru/CeO_2 and Ru/ZrO_2. It is noted that Ru particles on SnO_2 support did not adsorb CO after reduction treatment at 400 °C.

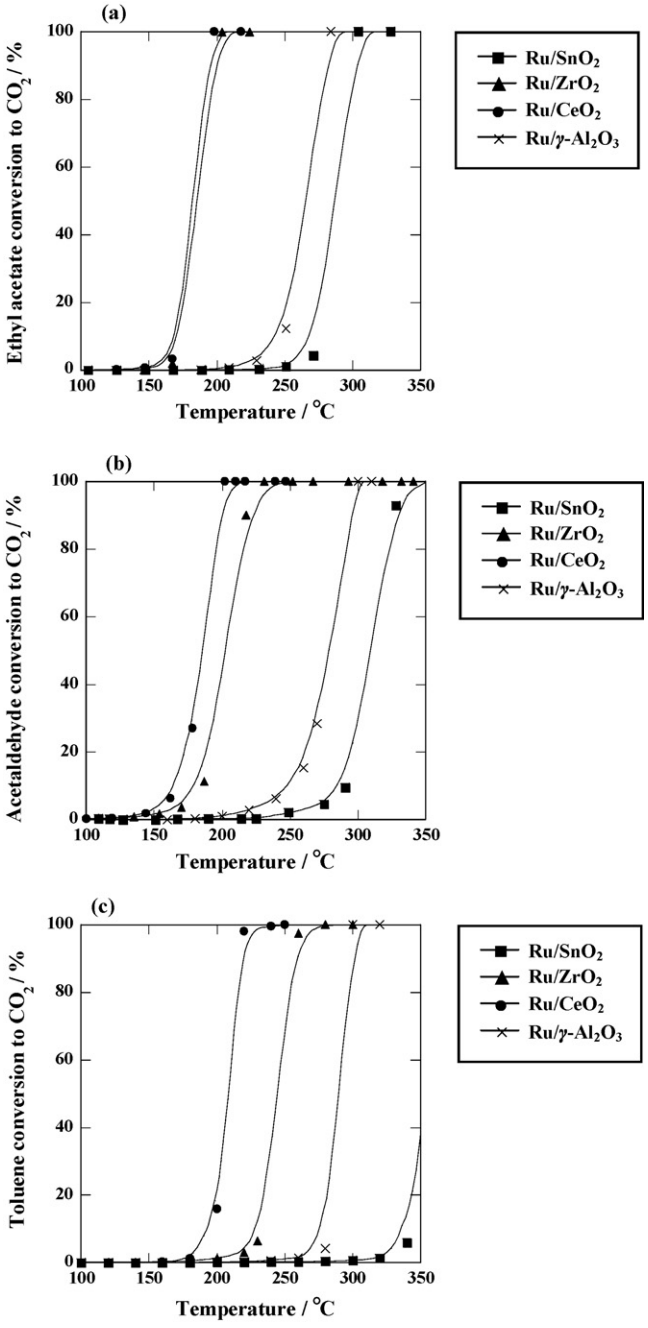

Fig. 2. VOC conversion as a function of temperature over supported 1.0 wt.% Ru catalysts reduced at 400 °C: (a) ethyl acetate, (b) acetaldehyde, and (c) toluene. Reaction conditions: VOCs, 1.0%; air, 99.0%; S.V. = 10,000 l kg^{-1} h^{-1}.

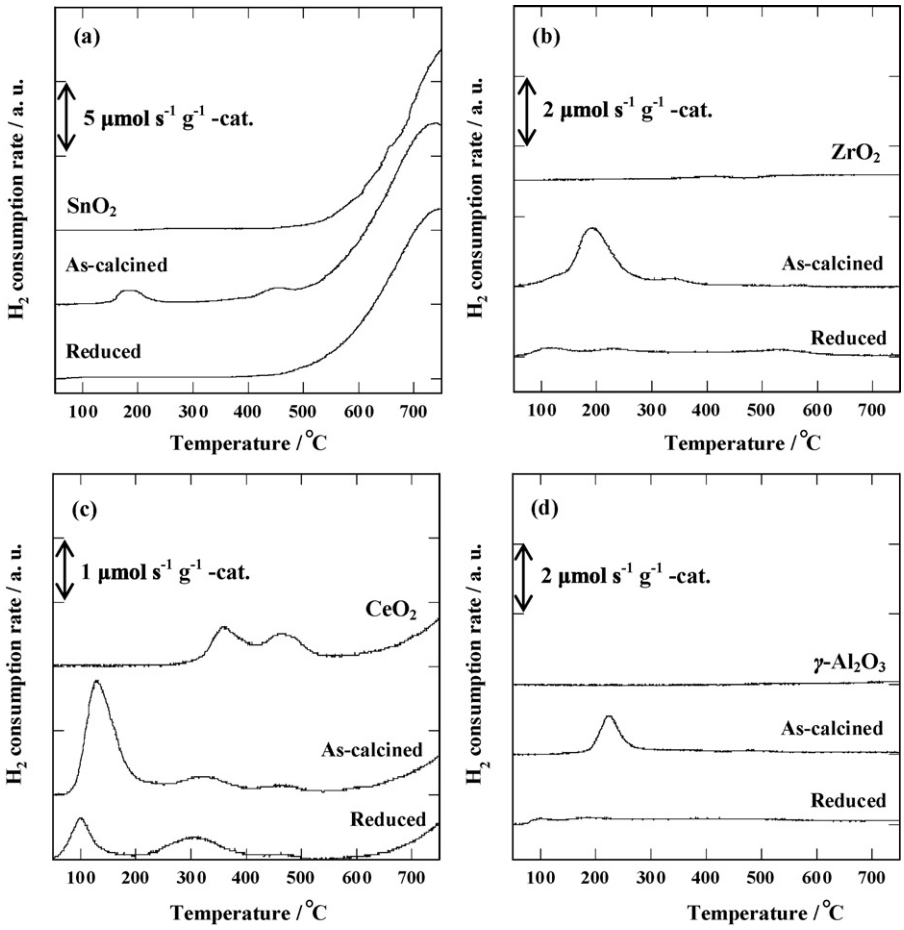

Fig. 3. Temperature-programmed reduction of supported 1.0 wt.% Ru catalysts: (a) Ru/SnO_2, (b) Ru/ZrO_2, (c) Ru/CeO_2, and (d) $Ru/\gamma\text{-}Al_2O_3$.

3.2.2. Temperature-programmed reduction

Temperature-programmed reduction profiles of the catalysts are shown in Fig. 3. The profile of as-calcined Ru/ZrO_2 and $Ru/\gamma\text{-}Al_2O_3$ showed a sharp peak at *ca.* 195 °C and 230 °C, respectively. These peaks were attributed to the reduction of ruthenium oxide, because the supports are almost irreducible in the temperature range. Furthermore, a broad peak appeared at *ca.* 340 °C for Ru/ZrO_2 due to the promoted support reduction through spillover of hydrogen species from Ru onto ZrO_2 [27,28]. In the case of as-calcined Ru/SnO_2, small two peaks were observed at *ca.* 195 and 450 °C. The former and latter peaks were corresponding to the reduction of ruthenium oxide and tin oxide surface in the vicinity of ruthenium particles, respectively. The latter reduction indicates the existence of strong chemical interaction between Ru and SnO_2. In addition, a broad peak attributable to the bulk reduction of tin oxide was observed above 500 °C. The profile of as-calcined Ru/CeO_2 consisted of three main peaks at low and high temperatures (130, 320, and 460 °C). The peak at *ca.* 130 °C corresponds to reduction of the ruthenium oxide, and the other two peaks at high temperatures are ascribed to the reduction of the surface capping oxygen of CeO_2 [29]. Consequently, the higher activity of Ru/CeO_2 should originate from ruthenium species reducible at the lowest temperature, as shown in Fig. 1. Ruthenium species reducible at lower temperatures should be responsible for VOC oxidation. The amount of H_2 consumption determined from the TPR profiles is summarized in Table 2. The amount of H_2 consumed over Ru/SnO_2 and $Ru/\gamma\text{-}Al_2O_3$ was almost comparable with the theoretical value (198 μmol g^{-1}) calculated by assuming the reduction of RuO_2 to Ru, whereas Ru/ZrO_2 and Ru/CeO_2 showed much larger hydrogen consumption.

In contrast, profiles of the reduced catalysts were quite different from those of as-calcined ones. Except for the reduced Ru/CeO_2, no reduction peak of ruthenium oxide appeared in TPR profiles, though all catalysts were exposed to air after the treatment in a hydrogen atmosphere. Thus, there exist ruthenium species on CeO_2 surface that are easily reduced and oxidized, and owing to such species both as-calcined and

Table 2
The amount of H_2 consumption determined from the reduction peak of ruthenium oxide in TPR profiles shown in Fig. 3

Sample	H_2 consumption (μmol g^{-1})
Ru/SnO_2	206
Ru/ZrO_2	669
Ru/CeO_2	565
$Ru/\gamma\text{-}Al_2O_3$	211

Theoretical value = 198 μmol g^{-1} ($RuO_2 + 2H_2 \rightarrow Ru + 2H_2O$).

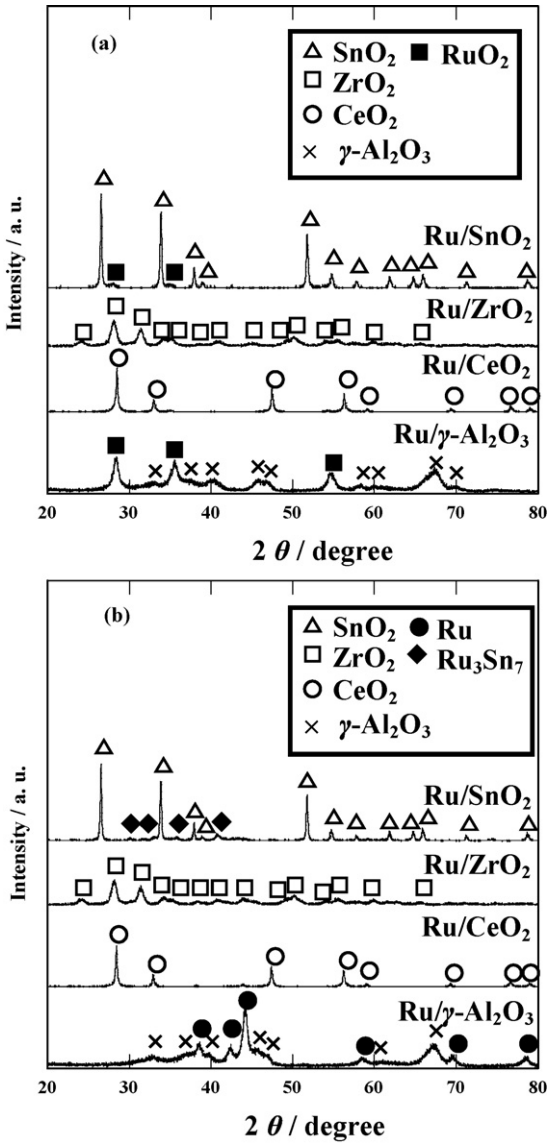

Fig. 4. XRD patterns of supported 10 wt.% Ru catalysts: (a) as-calcined and (b) reduced.

reduced Ru/CeO_2 showed similar activity as shown in Figs. 1 and 2.

3.2.3. X-ray diffraction

The XRD patterns of supported Ru catalysts before and after the reduction treatment are shown in Fig. 4. The diffraction patterns of as-calcined Ru/ZrO_2 and Ru/CeO_2 were consistent with those of ZrO_2 and CeO_2, respectively, with no lines ascribable to ruthenium species. Even after the reduction treatment, the patterns of these two catalysts are quite similar, suggesting that the size of ruthenium crystallites is too small to be detected [30]. In the case of $Ru/\gamma\text{-}Al_2O_3$, a new phase of metallic ruthenium was observed accompanied with disappearance of RuO_2 after the reduction treatment. This result can be attributed to lower degree of Ru dispersion on $\gamma\text{-}Al_2O_3$ surface (Table 1). On the other hand, the pattern of reduced Ru/SnO_2 was significantly changed. A new phase of intermetallic compound of Ru_3Sn_7 has appeared with a decrease of the intensity in SnO_2 line, indicating the solid-state reaction occurred between Ru and SnO_2.

Table 3
Binding energy of Ru $3d_{5/2}$ of the supported 10 wt.% Ru catalysts

Catalyst	Binding energy (eV)	
	As-calcined	Reduced
Ru/SnO_2	280.6	280.2
Ru/ZrO_2	280.8	279.8
Ru/CeO_2	280.7	279.6
$Ru/\gamma\text{-}Al_2O_3$	281.0	280.8

3.2.4. Surface analysis by XPS

The electronic state of ruthenium on supports was analyzed by XPS. All reduced catalysts were not exposed to air in this experiment. The binding energy of Ru $3d_{5/2}$ for supported Ru catalysts is summarized in Table 3. The energy of RuO_2 (Ru^{4+}) and metallic Ru (Ru^0) has been reported 280.7 and 280.1 eV, respectively, in the literature [31]. All reduced catalysts exhibited a slightly lower binding energy as compared with as-calcined catalysts, indicating that the ruthenium species was in reduced state.

The XPS spectra of the supports before and after reduction treatment are shown in Fig. 5. The spectra of Zr 3d and Al 2p were unchanged before and after reduction treatment. On the other hand, Ce 3d spectrum was significantly changed by reduction treatment. The XPS spectra of Ce 3d have been studied in detail [32–34]. In the spectrum of as-calcined sample, a peak (m_2) at 898.5 eV is attributed to the final state of $Ce(IV)3d^94f^0O2p^6$. The other peak of the state cannot be detected in high-binding energy (>910 eV). The doublet (m_1/n_1) at 889.9 and 907.4 eV is originated from the state of $Ce(IV)3d^94f^1O2p^5$, and the doublet (m_0/n_0) at 882.6 and 901.0 eV is corresponding to the state of $Ce(IV)3d^94f^2O2p^4$. In XPS spectrum of reduced sample, in contrast, other two pairs of spin-orbit doublets appeared. The doublet (v_0/u_0) at 880.3 and 898.7 eV is attributed to the state of $Ce(III)3d^94f^1O2p^6$, and the doublet (v_1/u_1) at 885.3 and 903.9 eV is assigned to the state of $Ce(III)3d^94f^2O2p^5$. These results indicate ceria is partially reduced by the reduction treatment. The spectra of Sn 3d were also strongly influenced by reduction treatment. The peaks at low- and high-binding energy are corresponding to Sn $3d_{5/2}$ and Sn $3d_{3/2}$ level, respectively. The spectrum of as-calcined sample exhibited a single peak at each orbital level, which is attributable to SnO_2. However, a shoulder peak appeared by reduction treatment, which was assigned to Sn^0 with the binding energy of Sn $3d_{5/2}$ = 485.0 eV and Sn $3d_{3/2}$ = 493.0 eV [31]. Thus, tin oxide was partially reduced by the reduction treatment, leading in the formation of intermetallic compound, Ru_3Sn_7.

3.2.5. Transmission electron microscopy

Fig. 6 shows TEM images of 1 wt.% Ru/SnO_2 before and after the reduction treatment. RuO_2 particles with the size of less than 10 nm were deposited on the SnO_2 surface after heating at 400 °C in air (Fig. 6(a)). A part of supported RuO_2

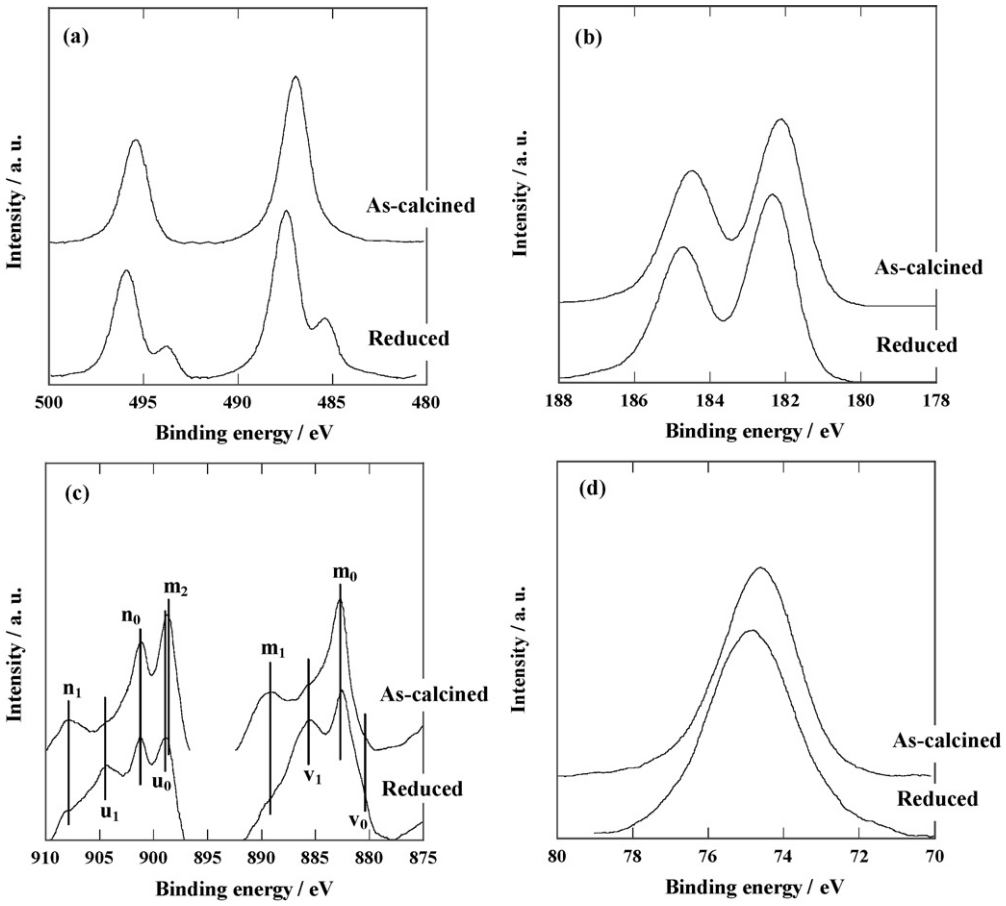

Fig. 5. XPS spectra of supported 10 wt.% Ru catalysts: (a) Sn 3d, (b) Zr 3d, (c) Ce 3d, and (d) Al 2p.

particles has a wetting morphology, indicating a strong interaction with SnO_2. On the other hand, the particle size of ruthenium increased and fine structure was changed into non-wetting state on the SnO_2 surface after reduction treatment at 400 °C in hydrogen. In addition, a peculiar nanostructure with core–shell morphology was formed (Fig. 6(c)). This core–shell structure cannot be observed right after the reduction treatment. Thus, the formation of the core–shell structure proceeds gradually in air, and is caused by oxidization of tin component at the most surfacial area of the intermetallic compound. The formation of the core–shell structure can deteriorate the catalytic activity for VOC combustion and the suppression of CO adsorption on the ruthenium surface. Similar specific phenomena induced by reduction treatment at 400 °C have been reported for other SnO_2-supported metal catalysts [17,35–37].

In general, since chemical interaction between ruthenium species and support is largely affected by the nature of the support materials, effect of the reduction treatment on the catalytic activity varied greatly, depending on the supports. When SnO_2 was used as support material, catalytic activity for VOC oxidation was significantly degraded by the reduction treatment due to the formation of the intermetallic compound with core–shell structure as shown in Fig. 6. This can be derived from a strong chemical interaction between Ru and SnO_2. On the other hand, catalytic activity of Ru/ZrO_2 and $Ru/\gamma\text{-}Al_2O_3$ was enhanced by the reduction treatment due to the formation of ruthenium in the metallic state. The ruthenium species on ZrO_2 surface were loaded in a highly dispersed state, resulting in a drastic enhancement of the catalytic activity, whereas the improvement over $\gamma\text{-}Al_2O_3$ support was not so distinct, possibly because of large particle size of ruthenium species on the $\gamma\text{-}Al_2O_3$ support. This indicates that the ruthenium particles have only a weak interaction with $\gamma\text{-}Al_2O_3$ support. In the case of CeO_2 support, Ru/CeO_2 exhibited the highest activity for all tests, which was almost unchanged before and after the reduction treatment. This can be because the reduced ruthenium species easily reacts with the lattice oxygen of CeO_2.

3.3. The stability of the reduced catalyst under reaction conditions

The durability of Ru/ZrO_2 reduced at 400 °C was evaluated, since the catalytic activity was significantly enhanced by the reduction treatment. First, three consecutive runs of ethyl acetate combustion were carried out. After the reaction temperature reached 250 °C, the ethyl acetate–air gaseous mixture was switched to pure nitrogen gas immediately, and the catalyst and reactor were cooled down to room temperature. Such operation was repeated. As shown in Fig. 7, the catalyst achieved the complete oxidation at low temperatures under atmosphere of a diluted VOC concentration. The high activity was maintained without deterioration throughout the operations.

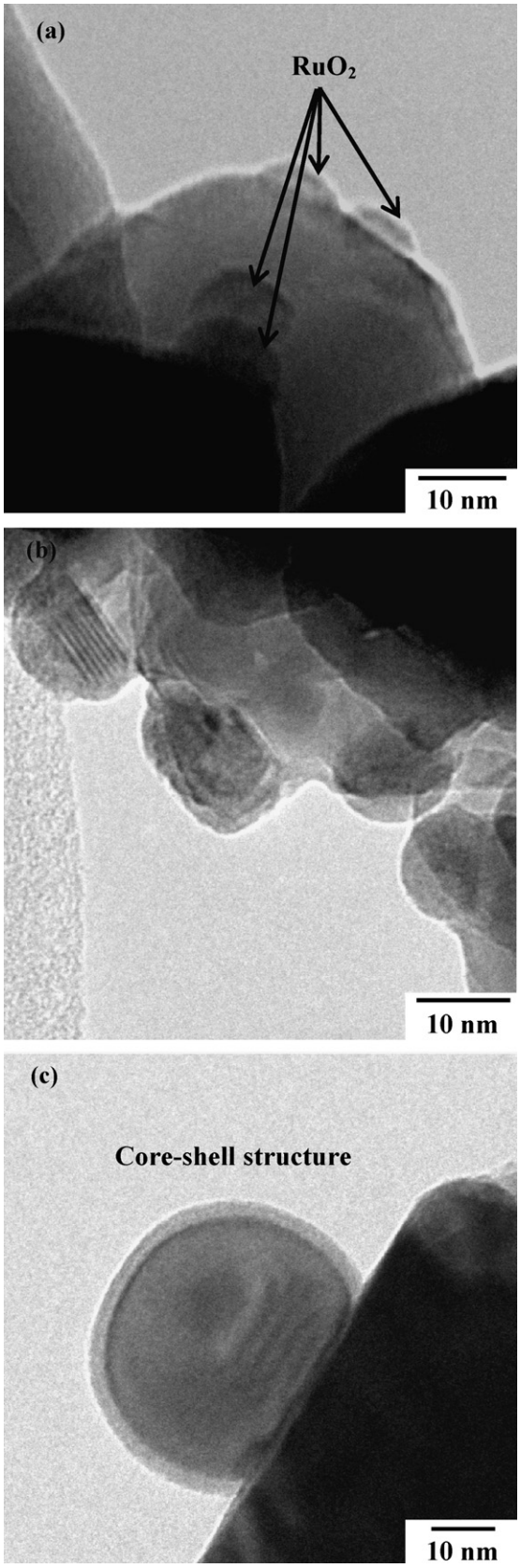

Fig. 6. TEM images of 1 wt.% Ru/SnO_2: (a) as-calcined and (b, c) reduced.

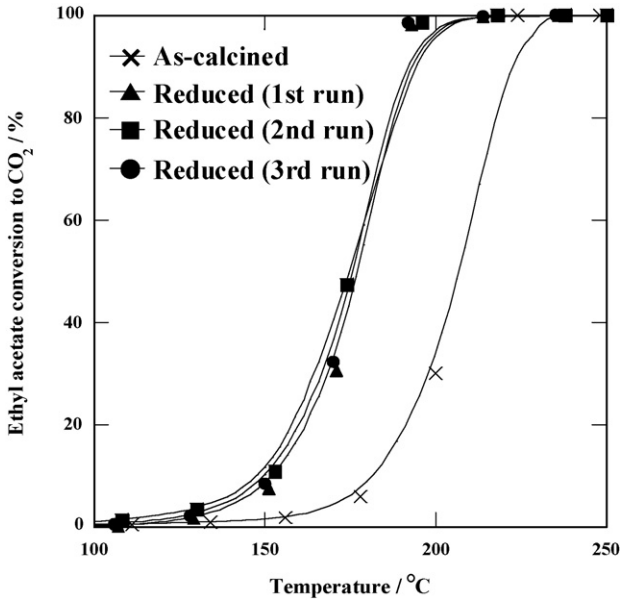

Fig. 7. Ethyl acetate conversion as a function of temperature over 1.0 wt.% Ru/ZrO_2 for sequential tests. Reaction conditions: ethyl acetate, 0.1%; air, 99.9%; S.V. = 10,000 l kg^{-1} h^{-1}.

Secondly, the influence of reoxidation treatment was studied. The reduced Ru/ZrO_2 was heat-treated at 200 or 400 °C for 30 min in air prior to catalytic reaction. The results are shown in Fig. 8. The high activity was also maintained irrespective of the re-oxidation treatment above 200 °C. Thus, the Ru species supported on ZrO_2 surface are stabilized in a reduced state with high dispersion even under the oxidizing atmosphere, resulting in the stable behavior during VOC combustion. The precious metals in metallic state should be responsible for the high-catalytic activity.

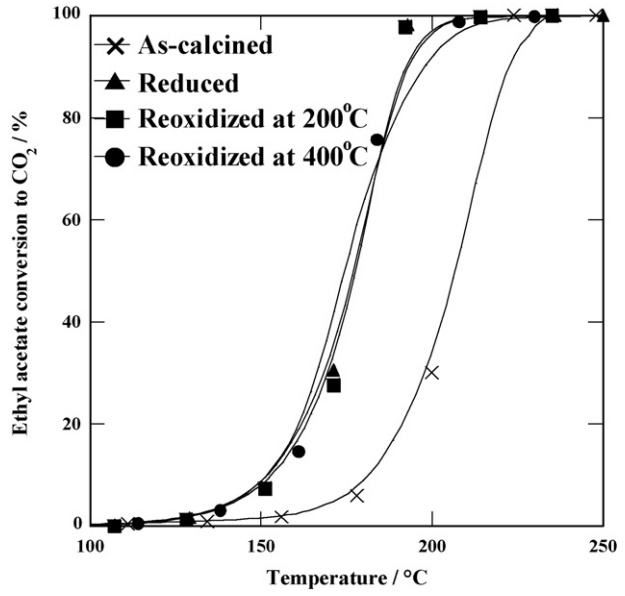

Fig. 8. Ethyl acetate conversion as a function of temperature over 1.0 wt.% Ru/ZrO_2 treated with calcinations in various conditions. Reaction conditions: ethyl acetate, 0.1%; air, 99.9%; S.V. = 10,000 l kg^{-1} h^{-1}.

4. Conclusions

Various oxide supported Ru catalysts were investigated for low-temperature oxidation of VOCs. A remarkable effect of the support was observed, and Ru/CeO_2 exhibited the highest activity for all tests regardless of the reduction treatment in hydrogen atmosphere. The redox species of ruthenium on CeO_2 with high dispersion should be responsible for the activity. This will be the useful design guide for low-temperature VOC oxidation. On the other hand, the catalytic activity of Ru/ZrO_2 and $Ru/\gamma\text{-}Al_2O_3$ was enhanced by the reduction treatment due to the formation of ruthenium in the metallic state. In the case of Ru/SnO_2, the formation of intermetallic compound with core–shell structure was confirmed, resulting in the deterioration of catalytic activity.

Acknowledgements

This study was supported by the Core Research for Evolutional Science and Technology (CREST) of the Japan Science and Technology agency (JST).

References

[1] B.J. Finlayson-Pitts, J.N. Pitts Jr., Science 276 (1997) 1045.
[2] Z. Meng, D. Dabdub, J.H. Seinfeld, Science 277 (1997) 116.
[3] R. Atkinson, J. Arey, Chem. Rev. 103 (2003) 4605.
[4] J.J. Spivey, Ind. Eng. Chem. Res. 26 (1987) 2165.
[5] V. Decottignies, L. Gasnot, J.F. Pauwels, Combust. Flame 130 (2002) 225.
[6] H. Einaga, S. Futamura, J. Catal. 227 (2004) 304.
[7] S.-W. Baek, J.-R. Kim, S.-K. Ihm, Catal. Today 93 (2004) 575.
[8] K. Faungnawakij, N. Sano, D. Yamamoto, T. Kanki, T. Charinpanitkul, W. Tanthapanichakoon, Chem. Eng. J. 103 (2004) 115.
[9] K. Faungnawakij, N. Sano, T. Charinpanitkul, W. Tanthapanichakoon, Environ. Sci. Technol. 40 (2006) 1622.
[10] M. Takeuchi, T. Kimura, M. Hidaka, D. Rakhmawaty, M. Anpo, J. Catal. 246 (2007) 235.
[11] K. Eguchi, H. Arai, Catal. Today 29 (1996) 379.
[12] E.M. Cordi, J.L. Falconer, J. Catal. 162 (1996) 104.
[13] P. Papaefthimiou, T. Ioannides, X.E. Verykios, Appl. Catal. B: Environ. 13 (1997) 175.
[14] K. Okumura, T. Kobayashi, H. Tanaka, M. Niwa, Appl. Catal. B: Environ. 44 (2003) 325.
[15] S. Ihm, Y. Jun, D. Kim, K. Jeong, Catal. Today 93 (2004) 149.
[16] N. Perkas, H. Rotter, L. Vradman, M.V. Landau, A. Gedanken, Langmuir 22 (2006) 7072.
[17] T. Mitsui, K. Tsutsui, T. Matsui, R. Kikuchi, K. Eguchi, Appl. Catal. B: Environ. 78 (2008) 158.
[18] A. Basińska, L. Kepiński, F. Domka, Appl. Catal. A: Gen. 183 (1999) 143.
[19] T. Utaka, T. Okanishi, T. Takeguchi, R. Kikuchi, K. Eguchi, Appl. Catal. A: Gen. 245 (2003) 343.
[20] A. Miyazaki, I. Balint, K. Aika, Y. Nakano, J. Catal. 204 (2001) 364.
[21] H. Bielawa, O. Hinrichsen, A. Birkner, M. Muhler, Angew. Chem. Int. Ed. 40 (2001) 1061.
[22] I. Balint, A. Miyazaki, K. Aika, J. Catal. 207 (2002) 66.
[23] J. Barbier Jr., L. Oliviero, B. Renard, D. Duprez, Catal. Today 75 (2002) 29.
[24] S. Hosokawa, H. Kanai, K. Utani, Y. Taniguchi, Y. Saito, S. Imamura, Appl. Catal. B: Environ. 45 (2003) 181.
[25] N. Li, C. Descorme, M. Besson, Appl. Catal. B: Environ. 71 (2007) 262.
[26] T. Takeguchi, S. Manabe, R. Kikuchi, K. Eguchi, T. Kanazawa, S. Matsumoto, W. Ueda, Appl. Catal. A: Gen. 293 (2005) 91.
[27] H. Ishikawa, J.N. Kondo, K. Domen, J. Phys. Chem. B 103 (1999) 3229.
[28] L.V. Mattos, F.B. Noronha, J. Power Sources 145 (2005) 10.
[29] H.C. Yao, Y.F. Yu Yao, J. Catal. 86 (1984) 254.
[30] N. Kamiuchi, T. Matsui, R. Kikuchi, K. Eguchi, J. Phys. Chem. C 111 (2007) 16470.
[31] J.F. Moulder, W.F. Stickle, P.E. Sobol, K.D. Bomben, in: J. Chastain (Ed.), Handbook of X-ray Photoelectron Spectroscopy, Perkin Elmer Corporation, Eden Prairie, MN, 1992.
[32] A. Pfau, K.D. Schierbaum, Surf. Sci. 321 (1994) 71.
[33] R. Leppelt, B. Schumacher, V. Plzak, M. Kinne, R.J. Behm, J. Catal. 244 (2006) 137.
[34] M. Abid, V. Paul-Boncour, R. Touroude, Appl. Catal. A: Gen. 297 (2006) 48.
[35] T. Takeguchi, T. Okanishi, S. Aoyama, J. Ueda, R. Kikuchi, K. Eguchi, Appl. Catal. A: Gen. 252 (2003) 205.
[36] T. Okanishi, T. Matsui, T. Takeguchi, R. Kikuchi, K. Eguchi, Appl. Catal. A: Gen. 298 (2006) 181.
[37] T. Matsui, T. Okanishi, K. Fujiwara, K. Tsutsui, R. Kikuchi, T. Takeguchi, K. Eguchi, Sci. Technol. Adv. Mater. 7 (2006) 524.